INSTITUTE OF PHYSICS PUBLISHING JOURNAL OF PHYSICS B: ATOMIC, MOLECULAR AND OPTICAL PHYSICS

J. Phys. B: At. Mol. Opt. Phys. **36** (2003) 1545–1558 PII: S0953-4075(03)54936-7

Differential partial ionization cross sections for 10–24 keV electrons colliding with helium and neon atoms

R K Singh and R Shanker[1]

Atomic Physics Laboratory, Physics Department, Banaras Hindu University, Varanasi 221005, India

E-mail: rshanker@banaras.ernet.in

Received 3 October 2002, in final form 18 February 2003
Published 3 April 2003
Online at stacks.iop.org/JPhysB/36/1545

Abstract

The relative differential partial ionization cross sections of helium and neon atoms for 10–24 keV electron impact have been measured by using an ejected electron–ion coincidence technique. Measurements were accomplished by employing a time-of-flight mass spectrometer for charge analysis of the ions and a channel electron multiplier working in a pulse-counting mode for detecting the slow electrons of non-discriminated energies ejected at 90° to the incident electron beam direction. The charge state fractions F_n of ions with charge states n are found to be nearly invariant with the impact energy. The present results show that the multiply charged ions of the target atoms are produced by different mechanisms, namely by a direct multiple ionization or by inner shell ionization followed by non-radiative transitions, for instance, by an Auger process combined with shake-off transitions. A good agreement is obtained between our experimental results and the calculations based on inner shell ionization cross sections folded with charge state abundances, which result from the decay of the corresponding initial inner shell vacancies.

1. Introduction

The relative abundances of multiply charged ions of noble gases have been studied extensively in mass spectrometers [1–5]. Many of these studies have been made at small impact energies and a small amount of information is available at higher energies. In recent investigations of multiple ionization of rare gases by electron impact, total and partial ionization cross sections (TPICS) have been measured by a number of workers [6–12]. Opal *et al* [13] and Oda *et al* [14] have measured the doubly differential cross sections, while Hippler *et al* [15] and Chaudhry *et al* [16, 17] have studied the partial doubly differential cross sections of ionization of the

[1] Author to whom any correspondence should be addressed.

0953-4075/03/081545+14$30.00

rare gas atoms. The cross-section data available in the electronvolt and low kiloelectronvolt energy range have usually contained a little information about ejected electrons from the given atomic shell or sub-shell; these electrons are generally produced as a result of direct ionization, Auger transitions and shake-off processes. In this effort, Hippler *et al* [15] and Chaudhry *et al* [16, 17] have obtained data at relatively low electron impacts. The maximum impact energies of 1.0 keV for argon [15] and 8 keV for xenon [16] for measuring the partial ionization cross sections, differential in energy and emission angle of the ejected electrons were used. No such data are available to our knowledge at the impact energies of the present experiments.

The work on helium and neon reported here is a continuation of our previous study on Ar [18]. It presents the experimental relative differential partial ionization cross sections (DPICS) for the multiply charged ions of He and Ne formed by 10–24 keV electrons incident on the target gases. The corresponding relative partial ionization cross sections have been deduced from the spectra produced by observing coincidences between the slow ejected electrons and the multiply charged target ions formed in the collisions. These cross sections have been normalized on the absolute gross ionization cross sections of Schram *et al* [19]. The advantage of using the present technique over the simple mass spectrometric or the condenser plate techniques has been explained in detail in our previous paper [18]. The present experiments were carried out on our recently developed set-up [20, 21] using an ejected electron-produced ion coincidence technique for a electron impact energy range of 10–24 keV.

In the present measurements, we are investigating the following collision reaction:

$$e_i^- + X \rightarrow X^{n+} + ne^- + e_s^- \tag{1}$$

where X and X^{n+} represent, respectively, neutral and n-fold ionized target atoms. e_i^- and e_s^- are, respectively, the incident and the scattered electrons, while e^- is the ejected (slow) electrons of relatively low energies. Detection of *slow* electrons at 90° to the incident beam direction in coincidence with the product X^{n+} ions yields the n-fold ionic charge state spectrum of the target atoms. In the present experiments, the detected electrons are considered to be predominantly the ejected ones of low energies from the target atoms compared to the scattered high energy primary electrons; the scattering angles of the primary scattered electrons remain confined to the small angles in the forward direction. The multiply charged ions produced in the collision reaction are analysed by a time-of-flight (TOF) set-up with the time delay of the order of a few microseconds, depending on the ionic charge state, mass and length of the drift tube of the TOF spectrometer, relative to the ejected electrons. In the present experiments, the resulting coincidence spectra correspond to those collision events from which the collision-induced target ions of a given charge state and the corresponding electrons of non-discriminated energies ejected at 90° to the incident electron beam direction are observed simultaneously. The acceptance angle of the channeltron for detecting the ejected electrons is determined to be $\Delta\theta_{ej} = 1.6°$. These measurements determine the DPICS of the multiply charged ions produced in the energetic collisions considered. Deduced results from these measurements are expected to add more detailed information on the collision-induced multiple ionization mechanism than to those which employ a simple mass-spectrometric technique to determine the different charged state ions, and to those which have used either the condenser plates or a pulsed beam-recoil ion coincidence technique. It may be mentioned here that the TPICS data, as obtained from a pulsed crossed beam-recoil ion coincidence technique or from a simple mass spectrometric method, can provide information on the relative charge state abundances and on the partial ionization cross sections of the target ions as they are inherently summed over the energy and emission angles of the ejected electrons from the ionizing events. The probability of detecting ions of particularly higher charge states may substantially differ for collision events in which *only* the 'produced ions' are detected, from that

in which the produced ions are detected simultaneously with the ejected electrons of varying energies and of a particular emission angle. In the latter case, the ejected electrons may have anisotropic angular distributions (see, e.g., [17]) for a particular charge state of the ions and it may indicate the presence of *non-dipole transitions*, say, for instance, the Auger transitions (which may exhibit anisotropy of the ejected electrons). If such a situation prevails, then the production of highly charged ions is expected more than that of *singly* charged ions. Furthermore, since our DPICS data have been obtained at only one ejected electron angle, namely, at $\theta_{ej} = 90°$, the deduced cross sections from the data cannot be compared on *one-to-one basis* with those of TPICS, but the relative DPICS are still comparable with the TPICS data of earlier workers under a brute assumption that the angular distributions of ejected electrons are approximately the same for different charge state ions. In such a comparison, one would expect to see a net effect of the difference between the two data; one obtained for TPICS and the other for DPICS. Our present experiments, in fact, show an indication of such non-dipole transitions for production of Ne^{2+} and Ne^{3+} ions (see section 3.4).

2. Experimental procedures

A detailed description of experimental set-up, optimization, performance, detection efficiency, timing resolution and precision involved with various components as well as of test results has been given in our earlier papers [18, 20, 21]. Only the main features of the experimental procedures which are important for the present measurements are summarized here. The schematic diagram of the present experimental set-up is shown in figure 1. We have used a custom-built electron source; beam energy can be varied between 2 and 50 keV. The accuracy of the beam energy at 24 keV is about 0.2%, while the beam diameter is less than 3 mm in the interaction region. Beam current used for the present measurements is always kept less than 0.1 nA and the base pressure of the reaction chamber is maintained at a pressure better than 1.5×10^{-6} Torr throughout the experiment.

The interaction zone is enclosed between two parallel plates of the TOF spectrometer, where the electron beam cross-fires a beam of neutral gaseous atoms (effusing through a multi-capillary tube having a diameter of 5 mm) at 90° with each other. From the interaction region, the electrons ejected at 90° to the incident electron beam direction are detected by a channel electron multiplier (CEM) with a small solid angle ($\sim 10^{-2}$ sr). Ions produced in the interaction zone are extracted by an electric field (160–190 V cm^{-1}) applied between the two condenser plates of the TOF spectrometer and finally detected by another CEM whose cone is biased at -3.5 kV. Both ion and electron signals derived from the respective detectors are processed with the standard NIM modules [18] and finally they are fed as START and STOP inputs to a time-to-amplitude converter (TAC). In the present measurements, the ion signal is used as a STOP signal while the electron signal is used as a START. The time delay (order of a few microseconds) between the arrivals of ejected electrons and that of product ions at their respective CEMs gives information about the charge states of the ions. A computer-based 4 K channel multi-channel analyser (MCA) is used for data acquisition, data management, stripping and plotting, etc.

When all components involving the coincidence set-up are made functional with their optimized values and ensuring the equal detection and transmission efficiencies of all charge states [18, 21], accumulation of the TOF spectra for a chosen target and incident electron energy is carried out on a computer-based MCA working in a pulse-height analysis (PHA) mode. We have recorded the TOF spectra for He and Ne, as shown in figures 2(a) and (b). The typical duration of data collection for a given impact energy varied from 3 to 5 h. The operating pressure in the present experiments is chosen to be 2.4×10^{-4} Torr, which ensures the *single*

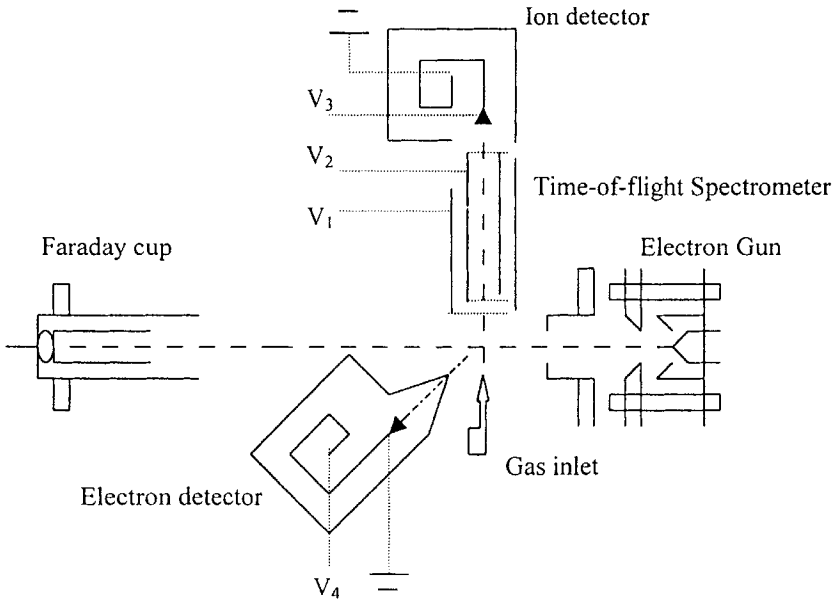

Figure 1. The schematic diagram of the multiple ionization experimental set-up. V_1–V_4 are various voltages applied to the ion and electron detectors.

collision condition [18]. The relative fractions of the produced ions in different charge states are deduced from the recorded spectra by integrating the pertinent target ion peaks (after the background subtraction, which is found to be uniformly distributed over the whole spectrum range) and normalizing the peak areas to the integrated charge counts of the beam current. The problem of residual gas contribution to the target ion peaks becomes serious when the residual gas ion peaks happen to coincide with the actual target ion peaks. Fortunately, in the present investigations, there are no residual gas-ion peaks present in the region of helium ion peaks; moreover, a clear separation between the H_2O^+ peak and Ne^+ is observed (see figure 2).

The uncertainty involved in the data of the present measurements is mainly due to the uncertainties in the beam current and in the data collection statistics. The typical contribution of the beam current uncertainty is about 1% and the statistical errors in data collection are generally less than 1% for singly charged ions; the latter uncertainties reach values of up to 18% for the higher charge states. Thus, the total uncertainties for Ne^+ (and He^+), Ne^{2+}, Ne^{3+} (and He^{2+}) are found to be about 1, 6 and ∼18%, respectively. These uncertainties are mostly within the size of the symbols used in the respective figures except for the highest charge states (e.g. He^{2+} and Ne^{3+}).

3. Results and discussion

3.1. Partial ionization cross sections

We have measured the partial ionization cross sections of helium and neon by impact of electrons with the incident energy range of 10–24 keV. The impact energy dependence of the partial ionization cross sections of He and Ne are shown in figures 3(a) and (b), respectively. No data from workers other than those from Schram *et al* [3] and from Van der Wiel *et al* [5] are available for comparison with our results in the investigated impact

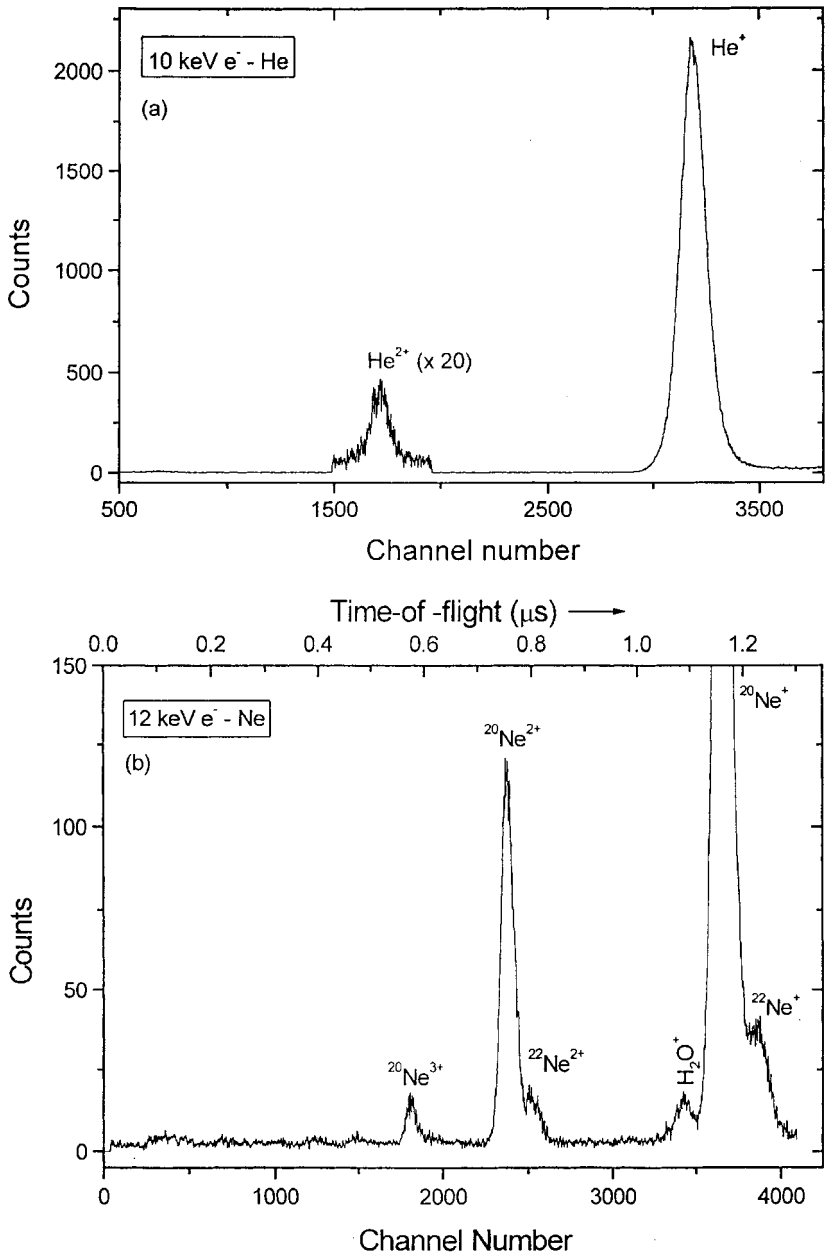

Figure 2. A typical TOF spectrum of He^{n+} ions (figure 2(a)) and Ne^{n+} ions (figure 2(b)). Spectra are recorded by observing the coincidences between helium ions and simultaneously ejected electrons of all energies at 90° with respect to the incident beam direction in a single collision condition.

energy range. The errors involved in evaluating the partial ionization cross sections of different charge states have been discussed in the earlier section. From figure 3, it is seen that the cross sections for different charge states of these atoms decrease gradually with impact energy and attain a value of about 50% of the cross sections obtained at 10 keV impact in the extreme

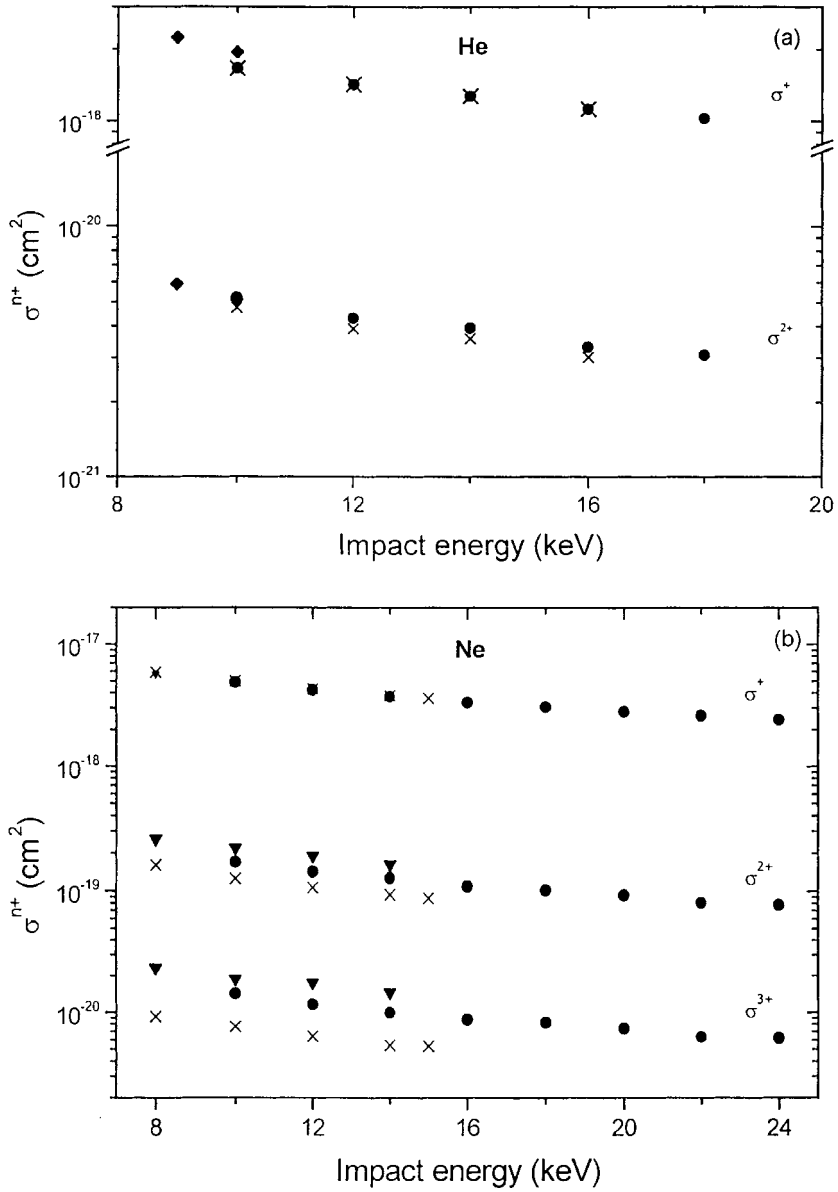

Figure 3. Energy dependence of partial ionization cross sections of helium (figure 3(a)) and neon (figure 3(b)) ●: present work; ×: [3]; ▼: [5]; ♦: [11].

higher side of the incident energy. No sudden change in the cross-section function is observed in any partial ionization data within the range of impact energy of investigation; because of the magnitudes of the ionization potential of the inner shell of Ne, for example (heavier than the helium atoms), Ne–K = 866 eV is much smaller than the impact energies (10–24 keV).

The single-ionization cross sections of neon obtained by Schram *et al* [3] are found to be in excellent agreement with our data, while the data on double- and triple-ionization cross sections of Ne from Schram *et al* are seen to be lower by about 5–20% in comparison to our data. On

the other hand, the data of Van der Wiel *et al* [5] for Ne^+ and Ne^{2+} ionization cross sections are found to be higher by about 15–36% as compared to our results (see figure 3(b)). Furthermore, our data for He^+ and He^{2+} ionization cross sections are seen to be in good agreement with those of Schram *et al* [3] within the experimental error of measurements. It is to be noted that there are no theoretical calculations available to compare with the present data.

3.2. Relative abundances

The relative fractions of different charge states (i.e. $R_1 = X^{2+}/X^+$ and $R_2 = X^{3+}/X^+$, where X = He, Ne) as a function of impact energy for helium and neon produced by electrons having impact energies from 10 to 24 keV are shown in figures 4(a) and (b), respectively. We have compared our results for relative charge state fractions with those of Schram *et al* [3], Van der Wiel *et al* [5], Andersen *et al* [22] and Shah *et al* [11]. These are the only results available in the literature for the electron impact energy range overlapping with the impact energies of the present investigation. In the case of He (see figure 4(a)), our values of R_1 are about 10–13% higher than the values of Schram *et al* and Shah *et al*. A close agreement is observed between the present results and those of Andersen *et al*, but the data of Van der Wiel are seen to overestimate the present results by about 50%. It is also noted from figure 4(a) that the ratio $R_1 = He^{2+}/He^+$, when plotted as a function of impact energy, is nearly constant around 0.3% and approaches a high velocity limit of 0.26% (see [9, 23]). Further, we have also compared our results for the ratio He^{2+}/He^+ with those of Muller *et al* [9] at a relativistic impact energy of electrons (40 MeV); in spite of a large difference in impact energies used in the two separate experiments, a remarkably good agreement is observed between the two results. This behaviour is explained in terms of a shake-off mechanism. Further, Ullrich *et al* [24] have suggested that the double ionization in helium is induced by only one single interaction of the projectile with one target electron (single ionization). The double ionization solely occurs due to the electron–electron interaction and the ratio R_1 is therefore extremely sensitive to the details of the time-dependent electron motion.

McGuire [25] has explained the double ionization of helium in terms of two mechanisms: shake-off and two-step process. In the shake-off mechanism, single ionization followed by final state rearrangement produces a doubly charged helium ion. This process is dominated at the higher velocity of incident electrons, where R_1 becomes independent of the incident velocity. In a two-step process, both electrons are ejected simultaneously as a result of the independent interaction with the projectile. McGuire shows that none of the above mechanisms explained the energy dependence of the double ionization of He for an entire impact energy range; however, the combination of shake-off and the two-step mechanism gives a plausible prediction for the experimental data. In the present investigation, R_1 is nearly independent of the impact energy; therefore, we believe that the production of doubly charged helium ions is mainly due to the shake-off process. Similar results have also been obtained by Knudsen *et al* [26] by the charged particle impact. They have shown that, for the light high velocity ions (H^+ and He^{2+}) compared to our electron velocities, the ratio R_1 becomes constant ($\sim 2.2 \times 10^{-3}$) and have concluded that only the one-step process, that is, the electron shake-off process, is responsible for double ionization of helium. This conclusion is also supported by the work of Carlson and Krause [27] for photoionization. If the ejected electrons are moving with high velocity (energy supplied to the electrons by photons is several times higher than its ionization energy), that is, the condition for the *sudden approximation* [27] is fulfilled, the probability for electron shake-off reaches an asymptotic value. In that case, the shake-off process is independent of the initial ionization mode and the ratio between double to single ionization obtains a constant value.

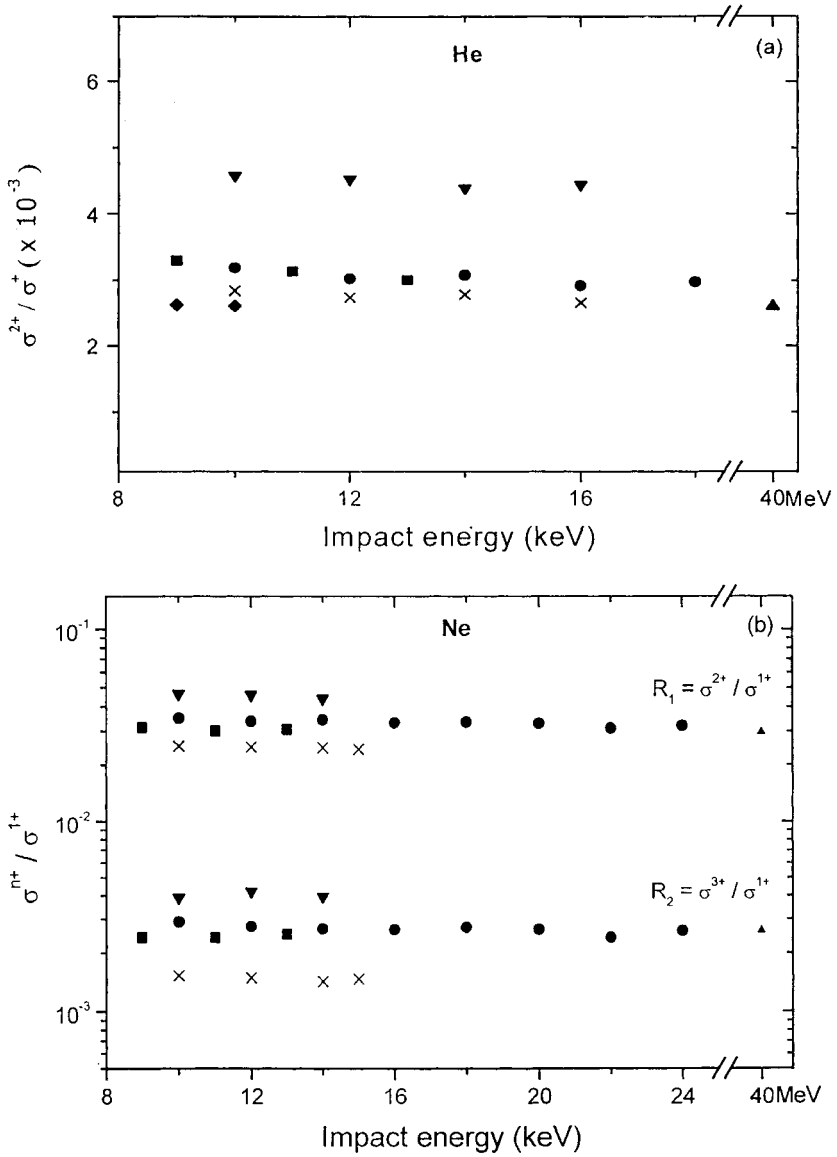

Figure 4. Relative fractions of different charge states (σ^{n+}/σ^{+}) for He (figure 4(a)) and Ne (figure 4(b)) as a function of impact energy. ●: present work; ×: [3]; ▼: [5]; ■: [22]; ▲: [9]; ♦: [11].

The situation is quite different for highly charged ion impact [28] where one should not expect to obtain the same value of the ratio R_1 as compared to that for electron impact. This discrepancy is mainly due to the varying shake-off contributions in double ionization of He. In ion–atom collisions, the sudden approximation does not apply fully. Instead, the dynamical correlations are important [22]. In this case mainly two 'two-step' processes are responsible for double ionization: firstly, an ejected electrons may collide with a second electron and eject it [29] and, secondly, a projectile may interact with both electrons [25, 29] especially for low

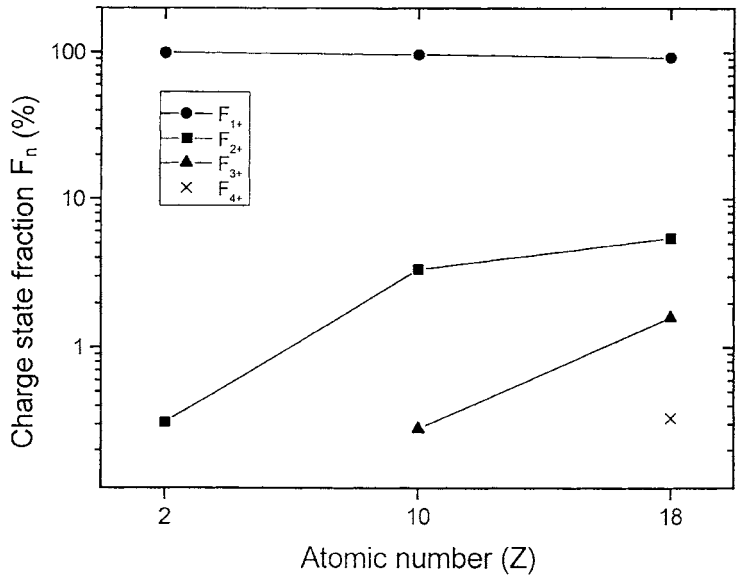

Figure 5. Variation of charge state fractions (F_n) of ions as a function of atomic number (Z). Lines connecting the data points are to guide the eyes.

impact energy. The first process is an important process at high impact energy, whereas the second process is vanishingly small in this case. The difference of e^- and positively charged ion (p^+) impact was studied first by McGuire [25] who has shown that the difference is mainly due to the charge effect rather than the mass effect. He suggested that this difference is due to interference between the two-step process and the shake-off process.

In the case of Ne, our values of R_1 and R_2 are found to be higher than those of Schram *et al* [3] by about 39 and 12%, respectively (see figure 4(b)). Again, our results are close to those of Andersen *et al* [22] in the overlapping region of impact energy. Figure 4(b) clearly shows that the ratios R_1 and R_2 are almost independent of the impact energy and remain relatively constant throughout the entire energy range and are in good agreement with the results of 40 MeV electron impact [9]. This shows that ratios of multiply to singly charged ions approach a value which is nearly energy independent at very high impact energies.

Andersen *et al* [22] have shown that the contribution of the K-shell for producing Ne^{2+} is very small [30, 31] for low energy proton impact, but for high energy ($\gg$10 MeV) proton impact, the double ionization of Ne may be produced by single ionization of the K-shell followed by a non-radiative decay. Here, it should be noted that, from analysis of the Ne Auger spectrum, it was ascertained that, when a K-vacancy is created by electron impact, it takes place by excitation about 2% of the time and by ionization for the remainder, for the 6.0 keV electron impact [32]. On the basis of the above discussions, we are of the view that the production of Ne^{2+} as well as of Ne^{3+} takes place mainly due to the creation of a K-shell vacancy followed by subsequent relaxations. This statement is strongly supported by the results of Kanngießer *et al* [33]. They have studied the coincidence spectrum of the ejected electrons from the K-shell of Ne and the ions produced by impact of 946 eV photons. From analysis of the spectrum, they found that, in these collisions, the K-shell vacancy is initially created which decays prominently by producing Ne^{2+} and Ne^{3+} ions via Auger or double Auger processes.

It is also noted that the values of F_{2+} and F_{3+} for Ar (see [18]) are relatively higher than those for Ne and He (see figure 5); this difference could be qualitatively understood in terms

of a large cloud of loosely bound outer shell electrons associated with Ar in comparison to that with He and Ne.

3.3. Charge state fractions

3.3.1. Theoretical consideration. From the knowledge of inner shell ionization and subsequent relaxation processes, it is possible to calculate the relative fractions of ions in different charge states at a given impact energy.

For calculating the charge state fractions, firstly, it is necessary to calculate the ionization cross sections of different atomic shells or sub-shells by electron impact. Hoffmann *et al* [34] have found a scaling behaviour of ionization cross sections for K, L and M shells of various atomic targets by relativistic electron impact. Their scaling law can be expressed in the form [35]

$$\sigma_\nu = \frac{\varepsilon_\nu}{I_\nu}\left[144.6\ln\left(\frac{E_e}{I_\nu}\right)+83\right]\mathrm{cm}^2\,\mathrm{keV}^{-1} \tag{2}$$

where σ_ν is the ionization cross section for the νth sub-shell, ε_ν is the number of equivalent electrons in the νth sub-shell, I_ν is the ionization potential of the νth sub-shell and E_e is the electron impact energy. Therefore, we can calculate the ionization cross sections of a single atomic sub-shell for the nth charge state following the relation [18]

$$\sigma_\nu^n = \sigma_\nu S_n(\nu) \tag{3}$$

and also the partial ionization cross sections given by

$$\sigma^n = \sum_\nu \sigma_\nu^n = \sum_\nu \sigma_\nu S_n(\nu) \tag{4}$$

where $S_n(\nu)$ are the relative abundances [36], n is the charge state and ν is the atomic sub-shell (i.e. K, L_1, $L_{2,3}$). Therefore, it is possible to calculate the relative charge state fractions and also the relative contributions of different sub-shells to produce the final charge state, that is,

$$F_n = \frac{\sigma^n}{\sum_n \sigma^n}, \qquad \text{and} \qquad F_{n,\nu} = \frac{\sigma_\nu^n}{\sum_n \sigma^n} \tag{5}$$

of the ions in different charge states n.

Another empirical formula which is most widely used for light ions in a kiloelectronvolt impact energy range (that is, in the case of non-relativistic collisions) is due to Lotz [37]:

$$\sigma_i = 4.5\times10^{-14}\sum_\nu \frac{\varepsilon_\nu}{I_\nu E_e}\ln\left(\frac{E_e}{I_\nu}\right). \tag{6}$$

3.3.2. Comparison with experiments. The present experimental results for charge state fractions of neon ions produced by electron impact at 10 keV as a function of their charge states are shown in figure 6. We have compared these results with those of Muller *et al* [9] for 40 MeV electron impact. The magnitude and structure of the present data are found to be in excellent agreement with the data of Muller *et al*.

Using equations (2)–(5) and Lotz's scaling formalism (6), we have calculated the charge state fractions of neon ions produced by 10 keV electrons. These calculations are compared with our experimental results (see figure 6). It is observed that the variation of the experimental *net* charge state fractions as a function of charge states is very similar to that of the theoretical calculations as shown by a thick line and the chain curves in the figure, respectively.

Further, figure 6 also includes the calculated values of relative charge state fractions $F_{n,\nu}$ from the respective partial cross sections σ_ν^n of different atomic sub-shells by using the

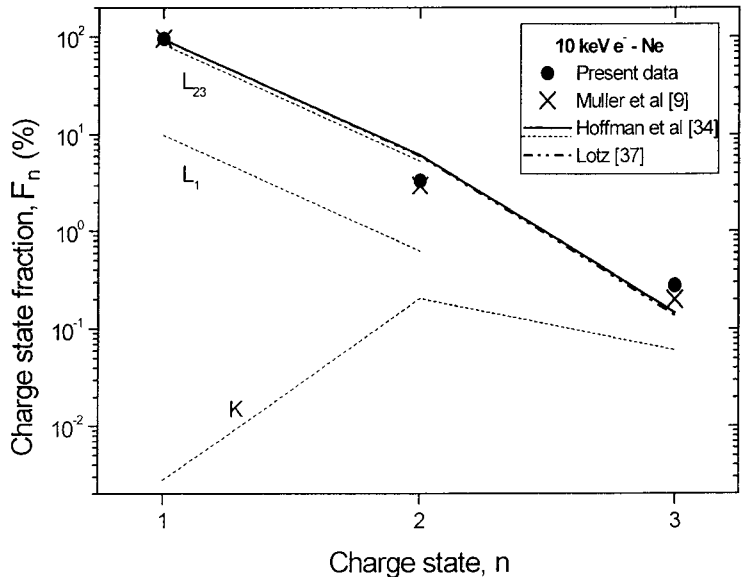

Figure 6. Comparison of the calculated and experimental data of the relative charge state fractions F_n for Ne^{n+} for 10 keV electron impact. Also shown are the calculated relative charge state fractions $F_{n,v}$ of the different sub-shells contributing to the production of ions in charge state n (broken lines).

relation (5). The possible contributions coming from different atomic shells or sub-shells to the net relative charge state fractions F_n are shown by dotted lines. This figure indicates that the production of Ne^+ is caused mainly due to the ionization of $L_{2,3}$ sub shells, while Ne^{3+} ions are formed dominantly due to the K-shell ionization followed by a subsequent atomic rearrangement.

3.4. Fano–Bethe plots

At high impact energies, Bethe theory [38] provides a good framework for analysing the ionization cross-section data. Bethe derived the expression for calculating the ionization cross sections of atoms induced by high energy electrons which can also be applied to calculate the partial ionization cross sections and is represented in the form [3]

$$\sigma_n = \frac{4\pi a_0^2 R}{E'_{el}} M_{in}^2 \ln c_{in} E'_{el} \tag{7}$$

where E'_{el} is the impact energy of the electrons with relativistic corrections. M_{in}^2 is the square of the dipole matrix element for optical transitions of an atom to a desired level including the continuum and c_{in} is a constant. In order to compare the present results with the theoretical calculations based on the Bethe–Born approximation, the graphs are plotted between $(\sigma_n E'_{el}/4\pi a_0^2 R)$ and $\ln E'_{el}$ (see equation (7)) as suggested by Fano [39]. Such plots yield straight lines; the slope of the lines give M_{in}^2, while the intercept gives $M_{in}^2 \ln c_{in}$.

Figures 7(a) and (b) show the Fano–Bethe plots for He^{n+} and $Ne^{n+}(n = 1–3)$ ions. It is observed that the singly charged ions exhibit a slightly positive slope for impact energies from 10 to 24 keV. These results show that the single-ionization cross sections of He and Ne are proportional to $E_{el}^{-1} \ln E'_{el}$ in accordance with the Bethe–Born approximation right up to an impact energy of 24 keV. Here, it is interesting to compare the present Fano plots of He^{2+} with

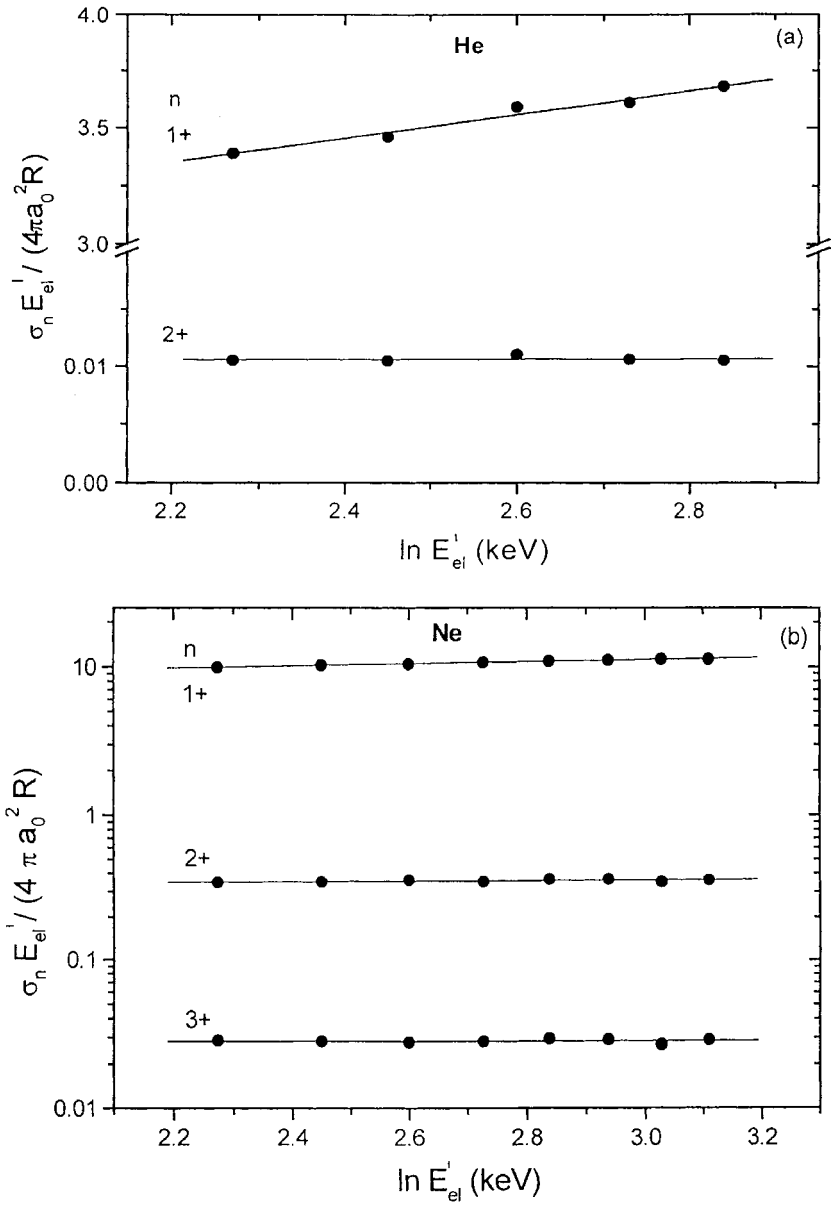

Figure 7. Fano–Bethe plots: $\sigma_n E'_{el}/4\pi a_0^2 R$ versus ln E'_{el} for different charge state ions of He (figure 7(a)) and Ne (figure 7(b)) produced by the impact of 10–24 keV electrons. Lines connecting the present data points are to guide the eyes.

the previous results of earlier workers. Schram *et al* [19] found the negative slope (which is in contradiction to the interpretation of the square of the dipole matrix element) while Nagy *et al* [7] presented the slight positive slope for the He^{2+}. In the present investigation, for He^{2+} as well as for Ne^{2+} and Ne^{3+}, the Fano–Bethe plots yield almost horizontal lines. The corresponding ionization cross sections are found to be proportional to E'_{el} within the statistical error of measurements. This feature is an obvious indication of the signature of disallowed

optical transitions, which are most likely responsible for producing these ions. It is therefore suggested that the higher charge states of ions produced in the collisions considered are mainly due to inner shell ionization followed by Auger transitions or by shake-off processes or by both.

4. Conclusions

The relative DPICS of He and Ne atoms by impact of 10–24 keV electrons have been measured by employing an ejected-electron-produced ion coincidence technique. The produced ions are analysed by using a TOF mass spectrometer while ejected electrons of non-discriminated energies ejected at 90° with respect to the electron beam direction are detected by a CEM operated in a pulse counting mode. The charge state fractions of the ions are found to be nearly invariant with the impact energy. The present results show that the multiply charged ions of the target gases are produced by both direct multiple ionization and by inner shell ionization followed by non-radiative transitions. A good agreement is obtained between our experimental results and the calculations based on inner shell ionization cross sections folded with charge state abundances which result from the decay of corresponding initial inner shell vacancies.

Acknowledgments

This work was supported by the Department of Science and Technology (DST), New Delhi under a research project No SP/S2/L-17/95. RKS wishes to thank the DST for awarding a research fellowship during progress of the work. The help received from R K Mohanta and S Mondal at different stages of the work is very much appreciated.

References

[1] Fiquet-Fayard F 1965 *J. Chim. Phys.* **62** 1065
[2] Stuber F A 1965 *J. Chem. Phys.* **42** 328
[3] Schram B L, Boerboom A J H and Kistemaker J 1966 *Physica* **32** 185
[4] Schram B L 1966 *Physica* **32** 197
[5] Van der Wiel M J, El-Sherbini T M and Vriens L 1969 *Physica* **42** 411
[6] Schmidt V, Sandner N and Kuntzemüller H 1976 *Phys. Rev.* A **13** 1743
[7] Nagy P, Skutlartz A and Schmidt V 1980 *J. Phys. B: At. Mol. Phys.* **13** 1249
[8] Stephan K, Helm H and Märk T D 1980 *J. Chem. Phys.* **73** 3763
[9] Muller A, Groh W, Kneissel U, Heil R, Ströhen H and Salzborn E 1983 *J. Phys. B: At. Mol. Phys.* **16** 2039
[10] Krishnakumar E and Srivastava S K 1988 *J. Phys. B: At. Mol. Opt. Phys.* **21** 1055
[11] Shah M B, Elliott D S, McCallion P and Gilbody H B 1988 *J. Phys. B: At. Mol. Opt. Phys.* **21** 2751
McCallion P, Shah M B and Gilbody H B 1992 *J. Phys. B: At. Mol. Opt. Phys.* **25** 1061
[12] Almeida D P, Fontes A C and Godinho C F L 1995 *J. Phys. B: At. Mol. Opt. Phys.* **28** 3335
[13] Opal C B, Beaty E C and Peterson W K 1972 *At. Data* **4** 209
[14] Oda N, Nishimura F and Tahira S 1972 *J. Phys. Soc. Japan* **33** 462
[15] Hippler R, Saeed K, Duncan A J and Kleinpoppen H 1984 *Phys. Rev.* A **30** 3328
[16] Chaudhry M A, Duncan A J, Hippler R and Kleinpoppen H 1987 *Phys. Rev. Lett.* **59** 2036
Chaudhry M A, Duncan A J, Hippler R and Kleinpoppen H 1989 *Phys. Rev.* A **39** 530
[17] Chaudhry M A, Duncan A J, Hippler R and Kleinpoppen H 1990 *Phys. Rev.* A **41** 4056
[18] Singh R K, Hippler R and Shanker R 2002 *J. Phys. B: At. Mol. Opt. Phys.* **35** 3243
[19] Schram B L, De Heer F J, Van der Wiel M J and Kistemaker J 1965 *Physica* **31** 94
[20] Singh R K, Mohanta R K, Hippler R and Shanker R 2002 *Pramana J. Phys.* **58** 499
[21] Singh R K, Mohanta R K, Singh M J, Hippler R, Goel S K and Shanker R 2002 *Pramana J. Phys.* **58** 623
[22] Andersen L H, Hvelplund P, Knudsen H, Moller S P and Sorensen A H 1987 *Phys. Rev.* A **36** 3612

[23] Ford A L and Reading J F 1988 *J. Phys. B: At. Mol. Opt. Phys.* **21** L685
[24] Ullrich J *et al* 1993 *Phys. Rev. Lett.* **71** 1697
[25] McGuire J H 1982 *Phys. Rev. Lett.* **49** 1153
[26] Knudsen H, Andersen L H, Hvelplund P, Astner G, Cederquist H, Danared H, Liljeby L and Rensfelt R-G 1984 *J. Phys. B: At. Mol. Phys.* **17** 3545
[27] Carlson T A and Krause M O 1965 *Phys. Rev.* A **140** 1057
[28] Berg H *et al* 1992 *J. Phys. B: At. Mol. Opt. Phys.* **25** 3655
[29] Andersen L H, Hvelplund P, Knudsen H, Møller S P, Elsener K, Rensfelt K-G and Uggerhøj E 1986 *Phys. Rev. Lett.* **57** 2147
[30] Eckhardt M and Schartner K H 1983 *Z. Phys.* A **312** 321
[31] Dubois R D and Manson S T 1987 *Phys. Rev.* A **35** 2007
[32] Carlson T A 1975 *Photo Electron and Auger Spectroscopy* (New York: Plenum) p 296
[33] Kanngießer B *et al* 2000 *Phys. Rev.* A **62** 014702
[34] Hoffmann D H H, Brendel C, Genz H, Low W, Muller S and Richter A 1979 *Z. Phys.* A **293** 187
[35] Brendel C, Genz H, Hoffmann D H H, Kuhn U, Low W, Seserko P and Richter A 1980 *Arbeitsbericht der Arbeitsgruppe Energiereiche Atomare Stosse* (Kassel: Gesamthochschule Kassel Fachbereich Physik) p 1
[36] Carlson T A, Hunt W E and Krause M O 1966 *Phys. Rev.* A **151** 41
[37] Lotz W 1968 *Z. Phys.* **216** 241
[38] Bethe H A 1930 *Ann. Phys., NY* **5** 325
[39] Fano U 1954 *Phys. Rev.* **95** 1198